Forced response of the El Niño–Southern Oscillation-Indian monsoon teleconnection in Earth System Models

Tamás Bódai[1,2], Mátyás Herein[3], Gábor Drótos[4], Valerio Lucarini[15,6], Frank Lunkeit[6]
[1]Center for Climate Physics, Institute for Basic Science, Korea, [2]Pusan National University, [3]Eötvös University Budapest, [4]Instituto de Física Interdisciplinar y Sistemas Complejos, [5]University of Reading, [6]University of Hamburg

- The ENSO has a global reach in shaping local weather, but affects tropical and subtropical regions the most [1].
- The teleconnection of the ENSO with the Asian monsoon systems has the greatest impact on human life, and severe episodes in the late XIX. century lead to the discovery of the ENSO [2].
- Under climate change what happens to the ENSO alone as well as its teleconnections is a much-studied and somewhat debated topic [3,4,5].
- The *response* of a system is defined by statistical mechanics in terms of an ensemble, which populates the so-called *snapshot/pullback attractor* [6].
- Via ergodicity the ensemble averages can be commuted with temporal averages in stationary systems.
- Under *nonstationarity* like climate change, while finite-time temporal averages of *global* average quantities might show negligible *ergodicity deficit* (difference from the ensemble average) [7], *local* quantities or teleconnections – a feature of *internal variability* – can be expected to feature much more ergodicity deficit [8].
- As a result of this, one can see "*false-trends*" in temporal average data, i.e., changes that are *not causal* consequences of the external forcing.
- We, therefore, for the first time, study the *ENSO-Indian monsoon (IM) teleconnection* in the correct ensemble-based framework, aiming to establish a causal connection between radiative forcing and the strength of the teleconnection **[9]**.
- Clearly, we cannot analyse observed data, because we have only *one Earth realisation*, but we use ensemble data generated by two Earth System Models (ESM); see Fig. 1.

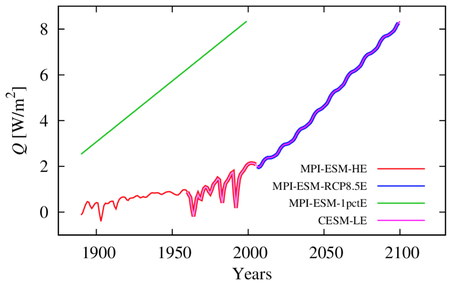

Fig. 1. (left above) *Nominal* [10] radiative forcing *Q* under historical forcing (HE) and future emission scenarios (RCP8.5E, 1pctE), and both (CESM-LE), presented to two ESMs studied: the Max Planck Institute ESM (MPI-ESM) and the Community Earth System Model (CESM) [11].

Fig. 2. (left below) ENSO-IM (p_{diff} vs P) teleconnection strength r for different forcings and ESMs.

Table 1. (below) p-values of statistical tests to detect nonstationarity in the response of the ENSO-IM (p_{diff} vs P) teleconnection.

	p_{KS0}	p_{KS1}	p_{KS2}	p_{t12}	p_{MK0}
MPI-ESM-HE	0.99	0.93	0.92	0.00020	0.000021
MPI-ESM RCP8.5E	0.75	0.28	0.93	0.76	0.58
MPI-ESM-1pctE	0.60	0.33	0.42	0.64	0.25
CESM-LE	0.83	0.68	0.99	0.072	0.20

Methodology and Results

- We represent the Indian monsoon by the JJA total precipitation *P* over North India (the box spanned by (31° N, 76° E), (31° N, 88° E), (17° N, 76° E), (17° N, 88° E)), and the ENSO by the JJA average pressure difference p_{diff} between Tahiti and Darwin (or: the Nino 3.4 index *T* based on sea surface temperature).
- We define the teleconnection as the Pearson's correlation coefficient; e.g.:

$$r = \frac{\langle p_{diff} P\rangle - \langle p_{diff}\rangle\langle P\rangle}{\sqrt{(\langle p_{diff}^2\rangle - \langle p_{diff}\rangle^2)(\langle P^2\rangle - \langle P\rangle^2)}}$$

- but we average <> over the ensemble members instead of time.
- Results for the forcings seen in Fig. 1 are shown in Fig. 2.
- Due to the *finite* ensemble size *N* fine details of the response are masked by noise, but even the nonstationarity is hard to see/detect. To this end, as a quantitative strategy, we deploy 3 different *statistical tests*: Kolmogorv-Smirnov (KS) tests, unpaired two-sample t-tests, Mann-Kendal (MK) tests; see results in Table 1.
- The applicability of the KS- and t-tests is due to the fact that the *Fisher transform z* of the Pearson's correlation coefficient *r*, $z = \arctan(r)$, follows approximately a *normal* distribution of standard deviation $1/\sqrt{N-3}$.

- We **find** (Table 1.) that nonstationarity cannot be detected by detecting nonnormality of the marginal distribution via the KS tests (p_{KS0}). The t-test (p_{t12}) and the alternative MK test (p_{MK0}), however, could detect nonstationarity in MPI-ESM-HE, but not in any other data set. This is surprising because the historical forcing is the *weakest*, and hints at the possibility that *Q* is *not a dynamical forcing*.
- Furthermore, further KS tests (p_{KS1}, p_{KS2}, results not shown) allow us to conclude that *r* ***increases*** from the first (1) to the second (2) half of the data set/XX. century. This is a finding seemingly ***opposing the scientific consensus*** that the strength of the ENSO-IM teleconnection was *decreasing* in the XX. century [12-16].
- We also confirm (Fig. 3) that temporal, as opposed to ensemble-wise', averaging in evaluating *r* leads typically to very significant false trends.

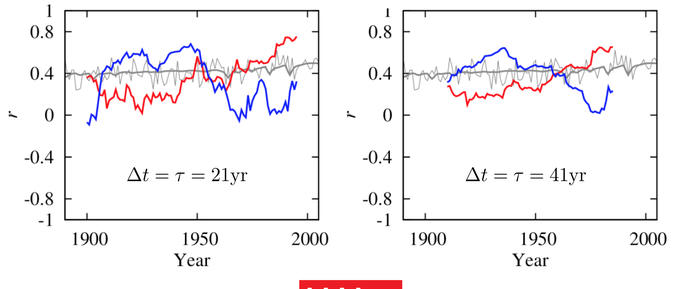

Fig. 3. (left) Time evolution of the ENSO-IM teleconnection, evaluating <> in the def' of *r* as *temporal* averaging in a time window of width Δt, in two realisations (red & blue) of the MPI-ESM-HE. Before calculating *r*, a *detrending* is done by subtracting from each data point of the time series a temporal average in a centred window of width τ. The ensemble-based result is also shown by the thin grey line.

Robustness wrt. four factors

- Model: CESM, MPI-ESM (Table 1, Fig. 2)

CESM doesn't even see much of a teleconnection, and shows no nonstationarity either even in the 20th c.

- Time window for MK test (Fig. 4).
- Quantity to represent ENSO: SOI (p_{diff}) or Nino3.4 (*T*) (Fig. 4).

Both seem to indicate a *nonmonotonic* nonstationarity, but there is a disagreement wrt. the *timing* of the change.

- Accounting for changes in patterns: via Canonical Corr' Analysis (CCA)

Both the correlations and their (PC1) changes are stronger.

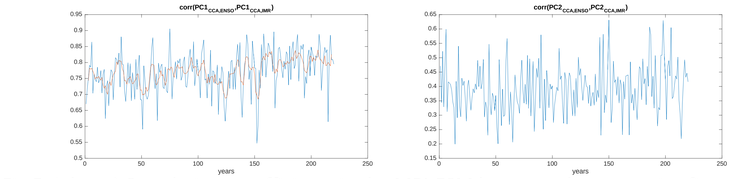

Fig.5. (above) Correlations coefficients in the MPI-ESM between the respective first (PC1, left) and second (PC2, right) modes identified by CCA.

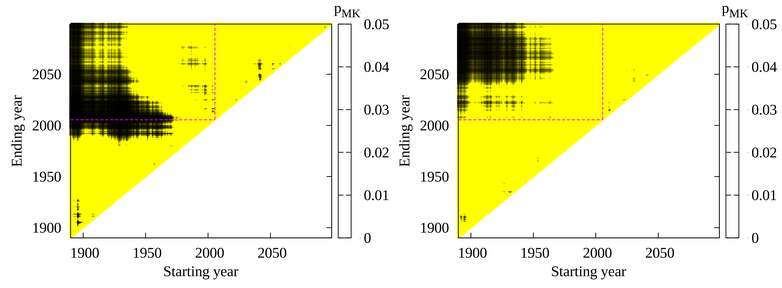

Fig. 4. (above) Detected nonstationarity of the teleconnection in the MPI-ESM via p-values of the Mann-Kendall test in time windows given by their start and end years. ENSO is represented by the SOI (p_{diff}, left) or the Nino3.4 index (*T*, right).

[1] Neelin, J. D. et al. (1998) J. Geophys. Res. Ocean. 103, 14261–14290. [2] Mike Davies. Late Victorian Holocaust, Verso (2000). [3] Guilyardi, E. et al. (2009) Bull. Am. Meteorol. Soc.90, 325–340. [4] Collins, M. et al. (2010) Nature Geoscience 3, 391 – 397. [5] Vecchi, G.A. and Wittenberg, A. (2010) WIREs Clim Change, 1, 260–270. [6] Drótos, G. et al. (2015) J. Climate 28, 3275–3288. [7] Drótos, G. et al. (2016) Phys. Rev. E 94, 022214. [8] Herein, M. et al. (2017) Sci. Rep. 7, 44529. **[9] Herein, M. et al. (2018) arXiv:1803.08909.** [10] Meinshausen, M. et al. (2011) Climatic Change 109, 213. [11] Kay et al. (2015) Bull. Amer. Meteor. Soc., 96:1333–1349. [12] Kumar, K.K. et al. (1999) Science 284:2156-2159. [13] Kinter, J.L. et al. (2002) J. Climate 15 , 1203–1215. [14] Ashrit, R.G. et al. Journal of the Meteorological Society of Japan. Ser. II, Released July 27, 2005. [15] Boschat, G. et al. (2012) Clim. Dyn. 38. 11, 2143-2165. [16] Chowdary, J.S. et al. (2012) J. Climate, 25, 1722–1744.